Tunneling and conformational flexibility play critical roles in the isomerization mechanism of vitamin D

Rubén Meana-Pañeda, and Antonio Fernández-Ramos*

Department of Physical Chemistry and Centro Singular de Investigación en Química Biolóxica e Materiales Moleculares (CIQUS), Faculty of Chemistry, University of Santiago de Compostela, 15782 Santiago de Compostela, Spain

Abstract

The thermal isomerization reaction converting previtamin D to vitamin D is an intramolecular [1,7]-sigmatropic hydrogen shift with antarafacial stereochemistry. We have studied the dynamics of this reaction by means of the variational transition state theory with multidimensional corrections for tunneling in both gas phase and n-hexane environments. Two issues that may have an important effect on the dynamics were analyzed in depth, i.e., the conformations of previtamin D and the quantum effects associated to the hydrogen transfer reaction. Of the large number of conformers of previtamin D that were located, there are sixteen that have the right disposition to react. The transition state structures associated to these reaction paths are very close in energy, so all of them should be taken into account for an accurate calculation of both the thermal rate constants and the kinetic isotope effects. This issue is particularly important because the contribution of each of the reaction paths to the total thermal rate constant is quite sensitive to the environment. The dynamics results confirm that tunneling plays an important role and that model systems that were considered previously to study the hydrogen shift reaction cannot mimic the complexity introduced by the flexibility of the rings of previtamin D. Finally, the characterization of the conformers of both previtamin D and vitamin D allowed the calculation of the thermal equilibrium constants of the isomerization process.

Introduction

Vitamin D is found in phytoplankton, which is one of the oldest forms of life. These organisms convert ergosterol (also called provitamin D_2) to previtamin D_2, when exposed to sunlight. After that previtamin D_2 isomerizes to vitamin D_2.[1,2] It seems that ergosterol helps to protect the organism from ultra-violet (UV) radiation, which can be harmful for the genetic code. From these early forms of life, vitamin D_2 passed to fish and from there, through the food chain to more evolved organisms, preserving most of its character. Of the two known forms of vitamin D for most of the mammals, including humans, the most active form of vitamin D is vitamin D_3, which differs from vitamin D_2 in the side chain of the sterol.

The deficiency of vitamin D leads to rickets, a common disease afflicting children during the nineteenth and the beginning of the twentieth centuries. The first studies on the subject pointed out the importance of taking cod-liver oil to prevent rickets[3] but it was in the 1920s that scientists realized that sunlight was essential for the production of vitamin D_3 by the body,[4,5] and that it promotes calcium deposition in the bones.[6] Vitamin D_3 is produced from 7-dehydrocholesterol, an sterol that is present in the skin of most higher animals, so vitamin D_3 is not really a vitamin, i.e., it is a substance that the body can manufacture and, therefore, its intake is not essential in the diet.[7–9] The production of the two forms of vitamin D follows the same mechanism, i.e., the sterol or provitamin D, which is already present in the organism, is transformed into previtamin D (Pre) by the action of UV radiation, which in turn thermally isomerizes to vitamin D (Vit), the thermodynamically most stable form of the two of them (see Scheme 1).

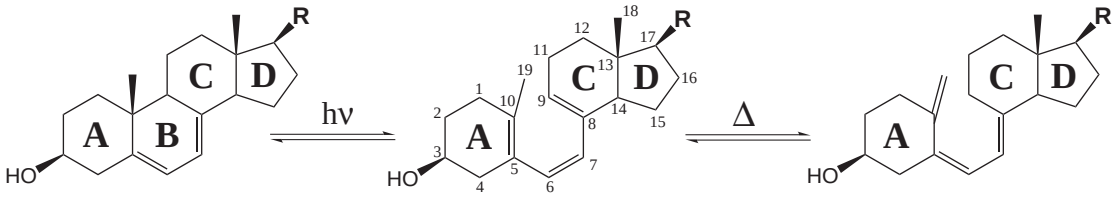

Provitamin D Previtamin D Vitamin D

Scheme 1

The action of the light not only affects the first step of the reaction, but also the thermal iso-

merization to Vit, because some side reactions are possible, i.e. the closure of the B ring leading to lumisterol or the rotation about the C_6-C_7 double bond (from Z to E) producing tachysterol. The production of these side products is reversible and it is possible due to the conformational flexibility of Pre.[10,11] The thermal isomerization of Vit occurs by a [1,7]-sigmatropic hydrogen shift when the C_5-C_6 and C_7-C_8 single bonds have s-cis conformations (cZc). From the experimental point of view it is not known which is the most stable form of Pre,[12] although the theoretical calculations point to the s-trans,s-cis conformer (tZc) as the one with the lowest energy.[13,14] The conformational analysis is complicated further by the flexibility of the A and C rings.

The thermal isomerization occurs with antarafacial stereochemistry.[16–18] However, there are two possibilities for antarafacial hydrogen exchange, i.e. the cis-10,6,8-triene can twist in a right-handed sense, i.e., the dihedral angle about the bond C_5-C_6 is positive (the A ring is below the C ring), so we call this configuration antarafacial(+), or it can be antarafacial(-), that is, the triene twists in a left-handed sense (the dihedral angle about the bond C_5-C_6 is negative), as shown in Scheme 2.

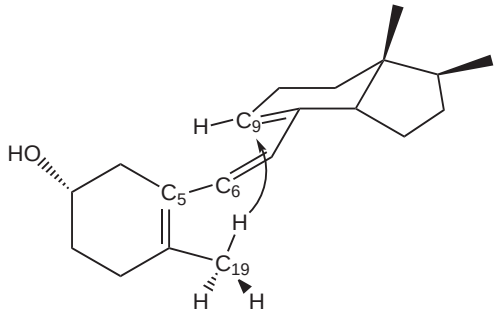

Antarafacial(+)

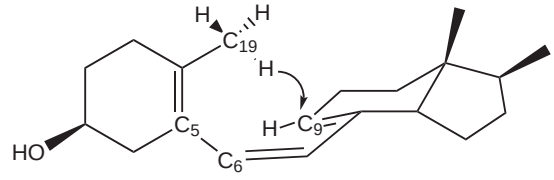

Antarafacial(-)

Scheme 2

Sheves et al.[19] using ^{2}H NMR and mass spectrometry techniques obtained that the hydrogen

shift prefers a right-handed disposition by a ratio of 2:1. Those authors also reported a kinetic isotope effect (KIE) for the isomerization in isooctane of about 45 at 80 °C. A more reliable value of the KIE was measured by Okamura et al.[20] using a pentadeuterio derivative of Pre in n-hexane, and at the same temperature of reaction obtained a KIE of 6.2. Baldwin and Reddy[21] reported a KIE of 7.0 for the 7-methylocta-1,3(Z),5(Z)-triene (see Scheme 3) at 60 °C (hereafter, we would refer to this triene simply as Tri); this KIE is very close to the value of 7.4 in Pre. The absolute value of the thermal rate constants are also close in value; 5.6×10^{-5} s^{-1} and 9.7×10^{-5} s^{-1} for Tri and for Pre, respectively. The similarity between the experimental data indicates that Tri could be a good theoretical model to study the isomerization reaction.[22,23]

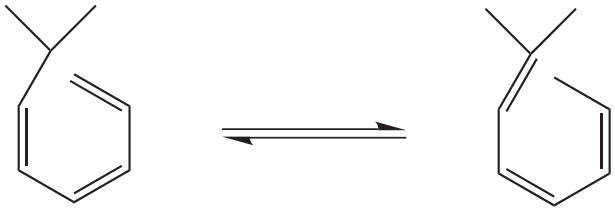

Scheme 3

Transition state theory[24] (TST) calculations carried out by Hess[22] on Tri at 60 °C led to a KIE of 3.9, which is almost half the experimental value. TST ignores quantum effects, but since the [1,7]-hydrogen shift is a hydrogen transfer reaction,[25] Hess indicated that the discrepancy between both KIEs may be due to quantum mechanical tunneling. In this context theoretical calculations based on variational transition state theory with multidimensional tunneling corrections[26] (VTST/MT) can be of great help because this theory incorporates quantum effects using semiclassical methods.[27–29] The VTST/MT calculations on Tri,[23] at 60 °C led to a KIE [1] of 5.5, which is in much better agreement with the experimental value, and therefore there is strong evidence that tunneling plays an important role in [1,7]-hydrogen shift reactions.

The agreement between the experimental data of Tri and Pre may hide important differences, because both the KIEs and the thermal rate constants are cumulative properties that may be due to

[1] KIEs calculated using TST are usually called quasiclassical, because do not include quantum effects (with the exception of the zero-point energy effects). On the other hand, KIEs calculated using VTST/MT are called semiclassical because quantum effects are incorporated semiclassically

the contribution of several reacting structures. In Tri there are several equilibrium conformations, but only one has the right structure to react, whereas in Pre we expect to have many reactive configurations due to the flexibility of the rings. In other words, should we expect a strong influence of the A and C rings in the isomerization reaction? How is this flexibility going to affect the thermal rate constants and the tunneling effect?

The objective of this work is to analyze in detail, from a theoretical point of view, the dynamics of the isomerization reaction of Pre to give an answer to the above questions. The rings bring complexity to the problem and, therefore, their incorporation is crucial for the understanding of the isomerization reaction. This is a difficult task due to the large size of the molecule, especially if the goal is to obtain accurate thermal rate constants and, thus, accurate KIEs. It can be achieved by interfacing electronic structure calculations and VTST/MT. The latter has proved to be a powerful tool for getting insight into reaction mechanisms of complex systems,[30] and the present work is pioneering the use of this approach to study the isomerization reaction in the Pre.

On the other hand, the thermal rate constants for the isomerization reaction have also been measured in anisotropic environments as the human skin,[31] liposomial models,[32] and $\beta-$cyclodextrins,[33] being the reaction more than 10 times faster than in n-hexane. Okamura et al.[20] Tian et al.[31] pointed out that a possible reason is that in human skin the amphipathic environment of the phospholipids would involve a larger participation of the antarafacial(-) attack.

To take into account the effect of the environment, we make a comparison of the gas-phase calculations with those obtained in n-hexane. The latter calculations also allow us to make a direct comparison with experiment.[20] The study of the isomerization reaction in anisotropic environments, as for instance the human skin, is out of the scope of this work. Still, we hypothesize about the mechanism of the process in these environments taking into account the previous experimental data and the results obtained in this work.

Calculation Method

The lateral chain (R in Scheme 1) distinguishes between the two forms of Pre (i.e. D_2 and D_3). It plays a major role in the transformation of Vit into a hormone, but at this stage of the process, in both the gas-phase and n-hexane environments, the lateral chain can be safely replaced by a methyl group, although we still preserve the names Pre and Vit to refer to these modified compounds.

All stationary-point geometries (equilibrium configurations and transition state structures) were optimized at the MPWB1K density functional method[34] with the 6-31+G(d,p) basis set.[35] This level of theory was already used in the study of the [1,7]-hydrogen shift in Tri with very good results, [23] and has shown to be adequate for nonmetallic thermochemical kinetics and thermochemistry.[36]

The experimental measurements on the isomerization reaction of Pre were carried out in n-hexane,[20] so in order to take into account the effect of the solvent, we have performed SM5.43R continuum solvation model[37] single-point calculations on the gas-phase MPWB1K/6-31+G(d,p) geometries at the MPW1K/6-31+G(d,p) level.[38] This solvation model has been extensively tested against experimental free energies of solvation for aqueous and organic solvents with good results.[37,39] The same type of calculations were carried out for the Tri system, so we could directly compare the [1,7] hydrogen shift in Pre and in Tri in this solvent.

In both, gas-phase and n-hexane environment, all the VTST/MT calculations were performed using canonical variational transition state theory (CVT),[40] and quantum effects were incorporated by the small-curvature tunneling (SCT) approach,[41] so hereafter, we refer to this methodology as CVT/SCT. Thermal rate constants were also calculated by TST for comparison. These calculations were also performed for the pentadeuterio derivative, Pre(d_5), isotopically substituted in the 9,14,19,19,19-positions, for which there are also experimental data available.[20]

The total isomerization rate constant should take into account all the paths that lead to reaction, so it can be considered as a multipath (MP) rate constant. The rate constants of interconversion between conformers are much faster than the individual isomerization rate constants, so the multipath rate constant can be obtained using the generalized version[42] of the Winstein-Holness equation[43]

(see Supporting Information). In this equation the multipath rate constant for isomerization using approximation Y (where Y = TST or CVT/SCT) can be written as the weighted sum of the individual isomerization reactions, i.e.,

$$k^{\mathrm{MP,Y}} = \sum_{i=1}^{n_{\mathrm{R}}} W_i(T) k_i^{\mathrm{Y}}(T) \tag{1}$$

where the weighting factor $W_i(T)$ is the statistical probability for the reaction occurring through path i, and n_{R} is the number of conformers that can lead to reaction. Computational details about the calculation of the CVT/SCT thermal rate constants, equilibrium constants and kinetic isotope effects for the isomerization process can be found in the Supporting Information.

All the electronic structure calculations were performed with *Gaussian03*,[44] the thermal rate constants were calculated with version 9.7 of the POLYRATE program.[45] The GAUSSRATE9.7[46] program made the linkage between the two packages. Free energies of solvation with the SM5.43R model were computed by a modified version of *Gaussian03* called Minnesota Gaussian Solvation Model (MN-GSM) version 2009.[47]

Results and Discussion

There are several aspect of the thermal isomerization reaction of Pre that need careful consideration, so we have divided the Section in several parts. In the first place we discuss the most relevant conformational aspects of the stationary points of reaction (a complete description of the conformations is given in the Supporting Information.) With this information about the conformers at hand it is straightforward to calculate the equilibrium constants. Finally we perform the dynamics calculations and obtain thermal rate constants and KIEs for the isomerization reaction in both gas phase and n-hexane. The results are also compared with those obtained for the [1,7] hydrogen shift reaction in Tri. The results on the statics and dynamics of the isomerization reaction were also used to get a hint about the same process in human skin and in other anisotropic environments.

Conformational Analysis

We have carried out an exhaustive conformational study of all the relevant stationary points (reactants, products and transition state structures) for the isomerization reaction. For the conformations of Pre we use the notation Pre_p(A,C)(±)qZ(±)r, where *p* indicates the position of the OH group: (a) for pseudo-axial, and (e) for pseudo-equatorial; the two possible configurations [half-chair (HC) or twist-boat (TB)] of the A and C cyclohexene rings is indicated in parentheses. The letters *p* and *q* indicate the s-cis or s-trans disposition of the dihedral angles about the C_5-C_6 and C_7-C_8 single bonds, respectively, i.e., s-cis (±)c for dihedral angles between 0° and ± 90°, and (±)t for dihedral angles between ± 91° and ± 180°. In Pre the C_6-C_7 double bond is always in *Z* configuration and the dihedral angle about the C_7-C_8 can only be (±)c due to steric impediments. Therefore, there are eight different conformations of the rings resulting from the combination of four conformations of the A ring with two conformations of the C ring. For each of the configurations of the rings, with the exception of $Pre_{a(\pm)}$(TB,HC) for which we could not locate any equilibrium structure, we have found five conformations by rotation about the single bonds. Of the five conformations, (+)c*Z*(+)c and (-)c*Z*(-)c are the equilibrium conformations for the antarafacial(+) and for the antarafacial(-) [1,7]-hydrogen shifts, respectively.[2] Therefore, we have found 35 conformations of which 14 of them are reactive. In the case of Vit in parentheses is indicated the configurations [chair (CH) or twisted (T)] of the A and C cyclohexane rings. The C_5-C_6 and C_7-C_8 double bonds are in *Z* and *E* configurations, respectively, whereas the C_6-C_7 single bond is labeled as (±)c or (±)t as in the Pre single bonds. For the 16 transition state structures [3] we use the same notation as for Pre, although the conformation of the rings would be intermediate between Pre and Vit. Table 1 lists the energetics of the stationary points for each of the sixteen reaction paths.

The relative stability of the equilibrium conformations are a result of the differences in energy between the conformations of the rings. Previous ab initio calculations indicated that HC is more

[2]The notation for the reactive configurations can be abridged, and for instance the conformation Pre_a(HC,TB)(+)cZ(+)c can be shortened to $Pre_{a(+)}$(HC,TB). Hereafter we use the latter when referring to reactive configurations.

[3]Although we could not locate the $Pre_{a(\pm)}$(HB,HC) reactive structures, we could locate the $TS_{a(\pm)}$(TB,HC) transition state structures.

stable than TB by about 5.5 kcal/mol in free cyclohexene,[48] and that CH is 4.3 kcal/mol more stable than T in 1,2-dimethylencyclohexane.[49] Thus the Pre(HC,HC) and Vit(CH,CH) configurations are roughly about 8 to 12 kcal/mol more stable than Pre(TB,TB) and Vit(T,T) configurations and about 4 to 6 kcal/mol than the Pre(HC,TB), Pre(TB,HC), Vit(T,CH) and Vit(CH,T) configurations. The differences in energy due to conformational changes are smaller in the transition state structures than in the equilibrium configurations and they are mainly related to the disposition of the C ring. The antarafacial(+) attack is favored by the HC C-ring conformation of Pre, whereas the antarafacial(-) is favored by the TB C-ring conformation of Pre, being of great importance in the stability of the transition states the final configuration of the C ring in Vit.

Thermodynamics Equilibrium Constants

Table 2 lists the calculated and experimental[20,31] equilibrium constants for the isomerization of the root species Pre(d_0) and of the pentadeuterio derivative Pre(d_5). The experimental equilibrium constants have been measured in n-hexane, and the comparison with the calculated values in the same solvent show that the stability of the Vit conformers is underestimated, although the calculations correctly predict the exoergodicity of the isomerization reaction. The equilibrium constants are completely determined by the set of Pre(HC,HC) conformers and by the two (axial and equatorial) Vit(HC,HC)ZtE conformers. The differences between the calculated gas-phase and n-hexane solvent equilibrium constants show that there is a high sensitivity of the isomerization reaction to the environment.

The above calculations and the conformational study of the equilibrium configurations of both Pre and Vit may be useful to qualitatively describe the magnitude of the equilibrium constants obtained by Holick and coworkers[31,33] in different anisotropic media. Those authors observed that at 37 °C the equilibrium constant varies from 1.76 in $\beta-$cyclodextrins to 11.44 in human skin. The large value of the equilibrium constant in human skin is similar to that obtained in liposomial models.[32] Holick and coworkers[31] pointed out that in the lipids there would be interactions that stabilize more the cZc conformers than the tZc conformers. These interaction would be a result of

the amphipathic (with both hydrophilic and hydrophobic parts) nature of both phospholipids and Pre. The OH group of Pre would form a hydrogen bond with the hydrophilic part of the lipid (the phosphoric acid) and the hydrophobic part of Pre would interact with the acyl chain of the lipid by intermolecular dispersion forces. However, to our understanding it is difficult to find a reason why these interactions should favor the cZc conformers over the tZc ones, and why this additional stabilization of the cZc form, if present, should increase the equilibrium constant. An easier explanation would be that the most stable conformers of Vit would be stabilized further by these amphipathic interactions. When the isomerization reaction takes place in the presence of $\beta-$cyclodextrins the equilibrium constant is near the unity. Cyclodextrins are a family of compounds made up of sugar molecules bound together in a ring, and in the case of $\beta-$cyclodextrins the diameter of the cavity is about 6.2 Å. The isomerization reaction takes place inside of a cavity formed by the complexation of two $\beta-$cyclodextrin molecules. This cavity may not be large enough to allow rotations about the C_5-C_6 (in the case of Pre) or the C_6-C_7 (in the case of Vit) single bonds. The disappearance of the tZc conformers of Pre and of the ZtE conformers of Vit would decrease the value of the equilibrium constant substantially.

These results show that the environment plays a very important role in the relative stabilities of the equilibrium structures of Pre and Vit, and that from the thermodynamics point of view the formation of Vit is not favored by solvation in non-polar organic solvents as n-hexane.

Thermal Rate Constants

The calculation of the thermal rate constants was carried out at several temperatures in the interval between 25°C to 95°C, but here we limit the analysis of the thermal rate constants to mainly two temperatures: $T = 37$°C (the normal body temperature), and $T = 60$°C,[4] one of the temperatures at which there are experimental results of thermal rate constants for the [1,7] hydrogen shift reaction of both Tri and Pre. The results at other temperatures can be found in the Supporting Information.

[4]The experimental temperatures are $T = 60.0$°C for Tri and $T = 60.10(\pm 10)$°C for Pre, respectively. The thermal rate constants for Pre were calculated at $T = 60.1$°C. However, in the text we use $T = 60$°C and make a direct comparison between the Tri and Pre results

Figure 1 plots the contribution in percentage of each of the reaction paths at 37 °C, and Table 3 lists the total thermal rate constants for the isomerization reaction. The solvent has the effect of lowering the total CVT/SCT thermal rate constants by 30% due to changes in the free energy of activation (22%), and to the decrease in the tunneling transmission coefficients (8%). It also has an important effect on the two major reaction paths (R1 and R5), because the solvent favors the pseudo-equatorial position of the OH group.[50] The rest of the channels increase the reactive flux by 26%. This percentage is not negligible and it shows that is important to seek for transition states coming from highly energetic (low populated) reactive conformers. The large number of reactive channels with low interconversion barriers between conformers may lead to situations in which there is hopping of reactive molecules between different channels. Variational transition state theory cannot account for these non-statistical effects, but to our understanding their impact on the thermal rate constants would be small. As an example, direct-dynamics simulations carried out for the isomerization reaction in cyclohexane confirmed the presence of important non-statistical effects.[51] However, even in that case the TST thermal rate constants were in excellent agreement with the experimental data.

Quantum effects are of great importance for the isomerization reaction, because at 37 °C tunneling increases the thermal rate constants by an order of magnitude. Most of the tunneling occurs very close to the top of the barrier, and at 37 °C for reaction path R1, the tunneling energy that contributes the most to the transmission coefficient (sometimes called representative tunneling energy[52]) is only 2.3 kcal/mol below the barrier. The SCT approximation describes well this type of situations in which tunneling trajectories do not deviate substantially from the classical path for reaction, and it has shown to perform well in other hydrogen shift reactions.[53] The SCT transmission coefficient for two major reaction paths diverge more than expected, i.e., 11.4 for R1 and 8.06 for R5, respectively (see Figure 2). This divergence can be traced down to the difference in stability between the chair and twisted conformations of Vit, because the least stable product has a wider reaction path.

Figure 3 shows that the multipath CVT/SCT thermal rate constants are in very good agreement

with the experimental data from ref 20. In n-hexane the antarafacial(+) attack at $T = 80^{\circ}$C contributes about 86%. This value is in agreement with experimental measurements of Sheves et al. [19] that showed that the antarafacial(+) attack is preferred, although our percentage is somewhat larger than the 67% predicted by those authors. Anisotropic microenvironments as the skin may accomodate better some of the conformers of Pre and their corresponding transition states than isotropic environments (as n-hexane), because Pre itself has some anisotropy with a hydrophilic hydroxyl group in the A ring when the rest of the molecule is hydrophobic. The stabilization of those highly energetic antarafacial(-) reactants with the C ring in twisted-boat form would not modify the contribution of reactants to the final rate constants, since that is dominated by the half-chair conformations. However, it may involve a substantial increase of the contribution of the transition states. For instance, an additional stabilization of these reactants and transition states with respect to the antarafacial(+) stationary points by about 1.7 kcal/mol would increase the thermal rate constants by roughly a factor of 3.

That is not the only possibility for increasing the thermal rate constants, since it may also happen that, in this environment, the most stable conformations of Pre would be less stabilized than the transition states. This may also happen in $\beta-$cyclodextrins, which catalyze the isomerization reaction becoming almost 5 times faster than in human skin at 37 $^{\circ}$C. In this case, as it was pointed out in the equilibrium constants Subsection, we believe that is the disappearance of both the tZc conformers of Pre and the ZtE conformers of Vit due to steric hindrance the ones that aid even more the reaction. This would lead to lower values of the equilibrium constants than in human skin, but to higher thermal rate constants, because the lowest conformations of Pre would be cZc, and the barrier heights for reaction would decrease.

The flexibility of the trienic system lowers the thermal rate constants for both Tri and Pre with respect to more rigid systems, because there is an expansion of the space of reactants. However, in Pre there is an additional flexibility due to the rings that leads to further expansion of the space of reactants but with an increase of reactivity that compensates it. Thus, at 60 $^{\circ}$C the sum of the reactive flux of all channels makes the multipath thermal rate constant of Pre about 50% higher

than the thermal rate constant of Tri. Another important difference between Pre and Tri is that for the latter the two possible antarafacial attacks lead always to transition states that are enantiomers and, therefore, each of them contributes 50%. In Pre this percentage may fluctuate depending on the environment. Table 3 shows that the rate constants of Pre are more affected by the environment than those of Tri, but, on the other hand, Tri would be be much less efficient than Pre in anisotropic media. This is an indication that higher sensitivity to the environment is related to more flexibility.

Kinetic Isotope Effects

The KIEs of each of the reaction paths (in n-hexane) with their contribution to the total KIE are plotted in Figure 4 at 37 °C. The gas-phase KIEs (not plotted) are slightly larger than those in n-hexane, and the total KIE is about 6% larger in n-hexane i.e. 7.62 versus 7.20. A comparison between Figure 2 and Figure 4 shows that transmission coefficients and the KIEs change in the same fashion, because the quasiclassical contribution to the individual KIEs varies much more uniformly than the tunneling contribution. As indicated in the porcentages of Figure 4 the two reaction paths that contribute the most to the final KIE are R1 and R5 and the individual KIES are 7.49 and 6.40, respectively. The total KIE (7.20) is somewhat larger than the average of these two values (6.95) due to the contribution of the other reaction paths (mainly R13 and R16), that have larger tunneling contributions to the KIE than these two reaction paths. In general, environments like n-hexane, that stabilize reaction path R5, would lead to lower KIEs than environments that preferentially stabilize R1, R13 or R16. From these data we point out that a good low-limit for the total KIE for the isomerization reaction is the individual KIE of reaction R5.

At 60 °C the experimental KIEs are 7.4 and 7.0 for Pre and Tri, respectively, whereas the theoretical calculations in n-hexane are 6.01 and 5.52, respectively. The agreement between them is reasonable (the theoretical KIEs are lower by about 20%) taking into account the incertainty in the experimental measuraments, especially in the thermal rate constants for the deuterium transfer (see Figure 3), and that we are using the harmonic-oscillator approximation, when there is some evidence that anharmonicity may have some influence in the value of the KIEs.[54]

Even when both systems have quite similar total KIEs, the partial KIE contributions are quite different. The quasiclassical contribution is larger in Tri, but the tunneling contribution is larger in Pre. In this case, the quasiclassical contribution to the KIE would be mainly due to vibration, so this contribution would be more important when the difference between the free energies of activation for the root and isotopically substituted species is large. As to the tunneling contribution to the KIE, it was expected to be larger for Pre than for Tri, because $\eta_{\text{tun}}(T)$ increases when the tunneling transmission coefficients are larger. This is consistent with a faster decay of the KIE for Pre than for Tri in the interval of temperatures between 25 and 95 °C.

Finally, we note that the R8, R12 and R16 reaction paths have large KIEs due to the tunneling contribution. Therefore, if in human skin the thermal rate constants are larger than in n-hexane due to an increase in the contribution of the antarafacial(-) attack, an experiment including measurements of the isotopically substituted Pre would display larger KIEs than those measured in n-hexane.

Concluding Remarks

We have carried out an exhaustive variational transition state theory theoretical study using the CVT/SCT approach on the [1,7] hydrogen shift reaction (or isomerization reaction) of Pre in both gas-phase and n-hexane environments. The conformational analysis of the equilibrium structures leads to a total of 35 conformers of Pre and to 24 conformers of Vit.

The great flexibility of the A and C rings leads to sixteen reaction paths for isomerization, and in both gas-phase and n-hexane environments the reaction occurs about 90% through antarafacial(+) attack. Although the contribution of the two of reaction paths obtained from the most stable configurations of Pre to the thermal rate constants and to the KIEs is substantial (about 74% at 37 °C), the contributions from some of the other reaction paths is relatively important and cannot be neglected. Therefore, the flexibility of the rings generates additional reactive flux. Besides, the contribution of these less important reaction paths increases the tunneling contribution as well as

the KIE. The narrow energy window in which the transition states were located makes the hydrogen shift reaction quite sensitive to the environment, and we suggest that a further stabilization of some of the transition states may be the reason for the isomerization reaction to be faster in human skin (anisotropic environment) than in n-hexane (isotropic environment).

The comparison between Pre and Tri shows that, although the trienic system is identical for both systems, their dynamics is quite different. Tunneling is more important in Pre than in Tri and for the former, in both gas phase and n-hexane environments, there is preference for the antarafacial(+) attack; a preference that cannot exist in Tri.

Acknowledgement

A. F.-R and R. M.-P. thank Centro de Supercomputación de Galicia (CESGA) and the Minnesota Supercomputing Institute for computer time.

Supporting Information Available

Computational details on the CVT/SCT thermal rate constants, the equivalence between the generalized Winstein-Holness equation and eq 1, the equilibrium constants, and the KIEs, are given in Section S.1. Section S.2 includes geometries and energetic parameters of all the relevant stationary points for the isomerization reaction. It also includes a discussion about the relative stability of the transition states, and some of the barriers for interconversion between conformers. Sections S.3 to S.6 have in common that list data at several temperatures between 298 and 400 K in both gas-phase and n-hexane environments, and for the Pre(d_0) and Pre(d_5) species: S.3 lists the total TST, CVT and CVT/SCT thermal rate constants. Section S.4 lists the SCT transmission coefficients and the contribution of each of the individual reaction paths to the total TST, CVT and CVT/SCT thermal rate constants. Section S.5 lists the total KIEs, and Section S.6 list the contribution of each of the reaction paths to the total KIEs. Section S.7 list the thermal rate constants and the KIEs of Tri in n-hexane. Complete refs 44 and 45 are given in Section S.8.

References

(1) Holick, M. F. In *Vetebrate Endocrinology: Fundamentals and Biomedical Implications*; Pang, P. K. T., Schreibman, M. P., Eds.; Academic Press: Orlando, FL, 1989; p 7.

(2) Holick, M. F. *J. Cell. Biochem.* **2003**, *88*, 296.

(3) Mellanby, E.; Cantag, M. D. *Lancet* **1919**, *196*, 407.

(4) Hess, A. F. *Am. J. Public Health* **1922**, *12*, 104.

(5) Goldblatt, H.; Soames, K. N. *Biochem. J.* **1923**, *17*, 294.

(6) McCollum, E. V.; Simmonds, N.; Becker, J. E.; Shipley, P. G. *J. Biol. Chem.* **1922**, *53*, 293.

(7) Rosenfeld, L. *Clin. Chem.* **1997**, *43*, 680.

(8) Holick, M. F.; Chen, T. C.; Lu, Z.; Sauter, E. *J. Bone Miner. Res.* **2007**, *22*, 28.

(9) Deluca, H. F. In *Vitamin D*; Feldman, D., Pike, J. W., Glorieux, F. H., Eds.; Elsevier, Inc.: Amsterdam, The Netherlands, 2005; Vol. 1, p 3.

(10) Jacobs, H. J. C.; Havinga, E. *Adv. Photochem.* **1979**, *11*, 305.

(11) Holick, M. F. In *Vitamin D*; Feldman, D., Pike, J. W., Glorieux, F. H., Eds.; Elsevier, Inc.: Amsterdam, The Netherlands, 2005; Vol. 1, p 37.

(12) Dauben, W. G.; Funhoff, D. J. H. *J. Org. Chem.* **1988**, *53*, 5376.

(13) Dauben, W. G.; Funhoff, D. J. H. *J. Org. Chem.* **1988**, *53*, 5370.

(14) Dmitrenko, O.; Frederick, J. H.; Reischl, W. *J. Photoch. Photobio. A* **2001**, *139*, 125.

(15) Schlatmann, J. L. M. A.; Pot, J.; Havinga, E. *Recl. Trav. Chim. Pays-Bas.* **1964**, *83*, 1173.

(16) Hess Jr., B. A.; Schaad, L. J.; Panciř, J. *J. Am. Chem. Soc.* **1985**, *107*, 149.

(17) Hoeger, C. A.; Okamura, W. H. *J. Am. Chem. Soc.* **1985**, *107*, 268.

(18) Hoeger, C. A.; Johnston, A. D.; Okamura, W. H. *J. Am. Chem. Soc.* **1987**, *109*, 4690.

(19) Sheves, M.; Berman, E.; Mazur, Y.; Zaretskii, Z. V. I. *J. Am. Chem. Soc.* **1979**, *101*, 1882.

(20) Okamura, W. H.; Elnagar, H. Y.; Ruther, M.; Dobreff, S. *J. Org. Chem.* **1993**, *58*, 600.

(21) Baldwin, J. E.; Reddy, P. *J. Am. Chem. Soc.* **1988**, *110*, 8223.

(22) Hess Jr., B. A. *J. Org. Chem.* **2001**, *66*, 5897.

(23) Mousavipour, S. H.; Fernández-Ramos, A.; Meana-Pañeda, R.; Martínez-Núñez, E.; Vázquez, S.; Ríos, M. A. *J. Phys. Chem. A* **2007**, *111*, 719; **2011**, *115*, 9322(E).

(24) Eyring, H. *J. Chem. Phys.* **1935**, *3*, 107.

(25) *Hydrogen-Transfer Reactions*; Hynes, J. T., Schowen, R. L., Klinman, J. P., Limbach, H. H., Eds.; Wiley-VCH Weinheim, 2007.

(26) Fernández-Ramos, A.; Ellingson, A.; Garrett, B. C.; Truhlar, D. G. *Rev. Comput. Chem.* **2007**, *23*, 125.

(27) (a) Hirschfelder, J. O.; Wigner, E. *J. Chem. Phys.* **1939**, *7*, 616; (b) Johnston, H. S. *Gas Phase Reaction Rate Theory*; Ronald Press, 1966; (c) Kuppermann, A. *J. Phys. Chem.* **1979**, *83*, 171.

(28) Truhlar, D. G.; Kupperman, A. *J. Am. Chem. Soc.* **1971**, *93*, 1840.

(29) Garrett, B. C.; Truhlar, D. G.; Grev, R. S.; Magnuson, A. W. *J. Phys. Chem.* **1980**, *84*, 1730.

(30) Pu, J.; Gao, J.; Truhlar, D. G. *Chem. Rev.* **2006**, *106*, 3140.

(31) Tian, X. Q.; Chen, T. C.; Matsuoka, L. Y.; Wortsman, J.; Holick, M. F. *J. Biol. Chem* **1993**, *268*, 14888.

(32) Tian, X. Q.; Holick, M. F. *J. Biol. Chem* **1999**, *274*, 4174.

(33) Tian, X. Q.; Holick, M. F. *J. Biol. Chem* **1995**, *270*, 8706.

(34) Zhao, Y.; Lynch, B. J.; Truhlar, D. G. *J. Phys. Chem A* **2004**, *108*, 6908.

(35) Hehre, W. J.; Ditchfield, R.; Pople, J. A. *J. Chem. Phys* **1972**, *56*, 2257.

(36) Zhao, Y.; Schultz, N. E.; Truhlar, D. G. *J. Chem. Theory Comput.* **2006**, *2*, 364.

(37) Thompson, J. D.; Cramer, C. J.; Truhlar, D. G. *J. Phys. Chem. A* **2004**, *108*, 6532.

(38) Lynch, B. J.; Fast, P. L.; Harris, M.; Truhlar, D. G. *J. Phys. Chem A* **2000**, *104*, 4811.

(39) Thompson, J. D.; Cramer, C. J.; Truhlar, D. G. *Theor. Chem. Acc.* **2005**, *113*, 107.

(40) Garrett, B. C.; Truhlar, D. G. *J. Chem. Phys.* **1979**, *70*, 1593.

(41) (a) Skodje, R. T.; Truhlar, D. G.; Garrett, B. C. *J. Phys. Chem.* **1981**, *85*, 3019; (b) Liu, Y.-P.; Lynch, G. C.; Truong, T. N.; Lu, D.-h.; Truhlar, D. G. *J. Am. Chem. Soc.* **1993**, *115*, 2408.

(42) Baldwin, J. E.; Raghavan, A. S.; Hess Jr., B. A.; Smentek, L. *J. Am. Chem. Soc.* **2006**, *128*, 14854.

(43) Winstein, S.; Holness, N. J. *J. Am. Chem. Soc.* **1955**, *77*, 5562.

(44) Frisch, M. J. et al. Gaussian03, Gaussian, Inc., Pittsburgh PA, (2003).

(45) Corchado, J. C. et al. POLYRATE−version 9.7, University of Minnesota, Minneapolis, (2007).

(46) Corchado, J. C.; Chuang, Y.-Y.; Coitiño, E. L.; Ellingson,; Zheng, J.; Truhlar, D. G. GAUSSRATE−version 9.7, University of Minnesota, Minneapolis, (2007).

(47) Marenich, A. V.; Kelly, C. P.; Thompson, J. D.; Hawkins, G. D.; Chambers, C. C.; Giesen, D. J.; Winget, P.; Cramer, C. J.; Truhlar, D. G. Minnesota Solvation Database–version 2009, University of Minnesota, Minneapolis (2009).

(48) Shishkina, S. V.; Shishkin, O. V.; Leszczynski, J. *Chem. Phys. Lett.* **2002**, *354*, 428.

(49) Hofmann, H.-J.; Cimiraglia, R. *J. Org. Chem.* **1990**, *55*, 2151.

(50) Lambert, J. B.; Marko, D. E. *J. Am. Chem. Soc.* **1985**, *107*, 7978.

(51) Kakhiani, K.; Lourderaj, U.; Hu, W.; Birney, D.; Hase, W. L. *J. Phys. Chem. A* **2009**, *113*, 4570.

(52) Kim, Y.; Truhlar, D. G.; Kreevoy, M. M. *J. Am. Chem. Soc.* **1991**, *113*, 7837.

(53) Shelton, G. R.; Hrovat, D. A.; Borden, W. T. *J. Am. Chem. Soc.* **2007**, *129*, 164.

(54) Wong, K. Y.; Richard, J. P.; Gao, J. *J. Am. Chem. Soc.* **2009**, *131*, 13963–13971.

Table 1: Relative values with respect to the Pre_a(HC,HC)(+)tZ(-)c conformer of classical energies (ΔE), classical energies including zero-point energy ($\Delta E(ZPE)$), standard-state free energies at 37°C in gas phase (ΔG_g^X) and in n-hexane (ΔG_s^X); X = R (in Pre), ‡ (in TS), and P (in Vit). All values are in kcal/mol

Reaction	Conformer	ΔE	$\Delta E(ZPE)$	$\Delta G_g^X(T = 37°C)$	$\Delta G_s^X(T = 37°C)$
	$Pre_{a(+)}$(HC,HC)	1.50	1.44	0.72	0.63
R1	$TS_{a(+)}$(HC,HC)	27.97	25.42	26.38	26.46
	$Vit_{a(+)}$(CH,CH)	1.83	2.24	2.32	2.74
	$Pre_{a(-)}$(HC,HC)	1.48	1.83	1.86	2.07
R2	$TS_{a(-)}$(HC,HC)	29.61	27.32	28.25	28.38
	$Vit_{a(-)}$(T,CH)	5.91	6.38	6.70	7.15
	$Pre_{a(+)}$(HC,TB)	6.02	6.16	5.25	5.26
R3	$TS_{a(+)}$(HC,TB)	31.32	28.79	29.63	29.70
	$Vit_{a(+)}$(CH,T)	7.32	7.09	6.43	6.88
	$Pre_{a(-)}$(HC,TB)	5.61	6.07	5.90	6.04
R4	$TS_{a(-)}$(HC,TB)	29.63	27.30	28.36	28.46
	$Vit_{a(-)}$(T,T)	9.76	10.65	10.98	11.18
	$Pre_{e(+)}$(HC,HC)	1.73	1.92	1.80	1.77
R5	$TS_{e(+)}$(HC,HC)	28.35	25.48	26.31	26.21
	$Vit_{e(+)}$(T,CH)	7.83	7.70	7.16	7.65
	$Pre_{e(-)}$(HC,HC)	2.87	2.93	2.54	2.47
R6	$TS_{e(-)}$(HC,HC)	30.28	27.60	28.39	28.31
	$Vit_{e(-)}$(CH,CH)	2.57	2.81	3.07	3.61
	$Pre_{e(+)}$(HC,TB)	6.85	6.83	6.30	6.15
R7	$TS_{e(+)}$(HC,TB)	31.60	29.07	29.89	29.77
	$Vit_{e(+)}$(T,T)	13.41	13.21	12.01	12.43
	$Pre_{e(-)}$(HC,TB)	6.99	7.10	6.56	6.48
R8	$TS_{e(-)}$(HC,TB)	30.47	28.07	29.09	28.98
	$Vit_{e(-)}$(CH,T)	6.20	6.67	6.76	7.17
	$Pre_{e(+)}$(TB,HC)	6.64	6.37	5.14	5.20
R9	$TS_{e(+)}$(TB,HC)	29.60	27.15	28.05	28.11
	$Vit_{e(+)}$(T,CH)	7.22	7.59	7.29	7.71
	$Pre_{e(-)}$(TB,HC)	7.54	7.33	6.22	6.27
R10	$TS_{e(-)}$(TB,HC)	31.73	29.41	30.38	30.52
	$Vit_{e(-)}$(T,CH)	7.27	7.85	7.92	8.49
	$Pre_{e(+)}$(TB,TB)	11.42	10.52	7.73	7.92
R11	$TS_{e(+)}$(TB,TB)	33.10	30.39	30.85	30.89
	$Vit_{e(+)}$(T,T)	12.40	12.37	11.57	11.97
	$Pre_{e(-)}$(TB,TB)	11.61	11.72	10.68	10.68
R12	$TS_{e(-)}$(TB,TB)	32.02	29.32	29.98	30.09
	$Vit_{e(-)}$(T,T)	10.42	10.61	9.98	10.52
	$Pre_{a(+)}$(TB,HC)	–	–	–	–
R13	$TS_{a(+)}$(TB,HC)	28.60	26.22	27.22	27.30
	$Vit_{a(+)}$(T,CH)	5.77	5.85	1.02	1.25
	$Pre_{a(-)}$(TB,HC)	–	–	–	–
R14	$TS_{a(-)}$(TB,HC)	29.46	27.10	28.02	28.20
	$Vit_{a(-)}$(T,CH)	5.55	6.23	6.40	6.65
	$Pre_{a(+)}$(TB,TB)	11.02	11.12	10.05	9.76
R15	$TS_{a(+)}$(TB,TB)	31.99	29.26	29.79	29.81
	$Vit_{a(+)}$(T,T)	10.59	10.86	10.51	11.11
	$Pre_{a(-)}$(TB,TB)	10.01	10.03	8.93	9.08
R16	$TS_{a(-)}$(TB,TB)	29.72	27.03	28.00	28.17
	$Vit_{a(-)}$(T,T)	8.79	9.45	9.29	9.59

Table 2: Calculated (in both gas phase $K_{eq,g}$ and in n-hexane $K_{eq,s}$), and experimental, K_{exp}, equilibrium constants for the root species, Pre(d_0), and for the pentadeuterated compound, Pre(d_5)

Molecule	T (°C)	$K_{eq,g}$	$K_{eq,s}$	K_{exp}[a]
Pre(d_0)	37.0	7.14	4.48	6.14[b], 6.22[c]
	60.0	5.42	3.49	4.12[b]
	60.1	5.42	3.49	5.37 ± 0.41
	69.35	4.89	3.19	4.53 ± 0.35
	74.35	4.64	3.04	4.17 ± 0.32
	79.9	4.38	2.88	3.82 ± 0.28
	85.5	4.13	2.74	3.51 ± 0.25
Pre(d_5)	60.5	6.12	3.98	5.42 ± 0.17
	69.7	5.54	3.64	4.66 ± 0.19
	74.1	5.29	3.49	4.36 ± 0.23
	80.4	4.96	3.29	3.99 ± 0.25
	85.5	4.72	3.15	3.72 ± 0.28

[a] From ref 20 if not indicated otherwise.
[b] From ref 31.
[c] From ref 33.

Table 3: Calculated and experimental thermal rate constants (in s^{-1}) for the [1,7] hydrogen and deuterium shifts in Pre and Tri, respectively. The deuterated derivatives have been isotopically substituted in the 9,14,19,19,19-positions in Pre, and in the 7-position in Tri

	Pre ($T = 37°$C)		Pre ($T = 60°$C)		Tri ($T = 60°$C)	
	H	D	H	D	H	D
Rate constant			Gas phase			
k^{TST}	1.18×10^{-6}	3.46×10^{-7}	1.87×10^{-5}	5.91×10^{-6}	1.02×10^{-5}	2.60×10^{-6}
k^{CVT}	1.18×10^{-6}	3.42×10^{-7}	1.85×10^{-5}	5.84×10^{-6}	1.00×10^{-5}	2.60×10^{-6}
$k^{\mathrm{CVT/SCT}}$	1.27×10^{-5}	1.67×10^{-6}	1.39×10^{-4}	2.21×10^{-5}	4.80×10^{-5}	8.72×10^{-6}
			Solution			
k^{TST}	9.09×10^{-7}	2.67×10^{-7}	1.44×10^{-5}	4.59×10^{-6}	1.10×10^{-5}	2.80×10^{-6}
k^{CVT}	9.00×10^{-7}	2.64×10^{-7}	1.42×10^{-5}	4.54×10^{-6}	1.08×10^{-5}	2.80×10^{-6}
$k^{\mathrm{CVT/SCT}}$	9.00×10^{-6}	1.25×10^{-6}	1.01×10^{-4}	1.67×10^{-5}	5.17×10^{-5}	9.37×10^{-6}
k_{exp}	6.8×10^{-6} [a]	—	$9.72(\pm 0.03)\times10^{-5}$ [b]	$1.32(\pm 0.034)\times10^{-5}$ [b]	5.6×10^{-5} [c]	8.0×10^{-6} [c]
			6.76×10^{-5} [a]			

[a] From ref 31.

[b] From ref 20. The experimental temperatures are $T = 60.10(\pm10)°$C and $T = 60.50(\pm10)°$C for Pre(d_0) and Pre(d_5), respectively. The TST and CVT/SCT thermal rate constants listed in this Table were calculated at the experimental temperatures.

[c] From ref 21

Figure Captions

Figure 1: Histogram plotting the contributions of each of the individual reaction paths (Y=TST or CVT/SCT) to the total total rate constant in both gas-phase and n-hexane solution at $T = 37°$C.

Figure 2: Histogram plotting the SCT transmission coefficients obtained in n-hexane for all the reactive channels at $T = 37°$C.

Figure 3: Arrhenius plot that compares experimental and multipath CVT/SCT thermal rate constants in n-hexane for both Pre(d_0) and Pre(d_5).

Figure 4: Histogram plotting the quasiclassical, η_{qc}, and quantum, η_{tun}, contributions of each of the isomerization reaction paths of Pre to the total KIE at $T = 37°$C. The contribution in percentage, $\%\eta_i$, of each of the paths to the final KIE is indicated next to the bars. The resulting quasiclassical, quantum and total KIEs are plotted in the last three rows.

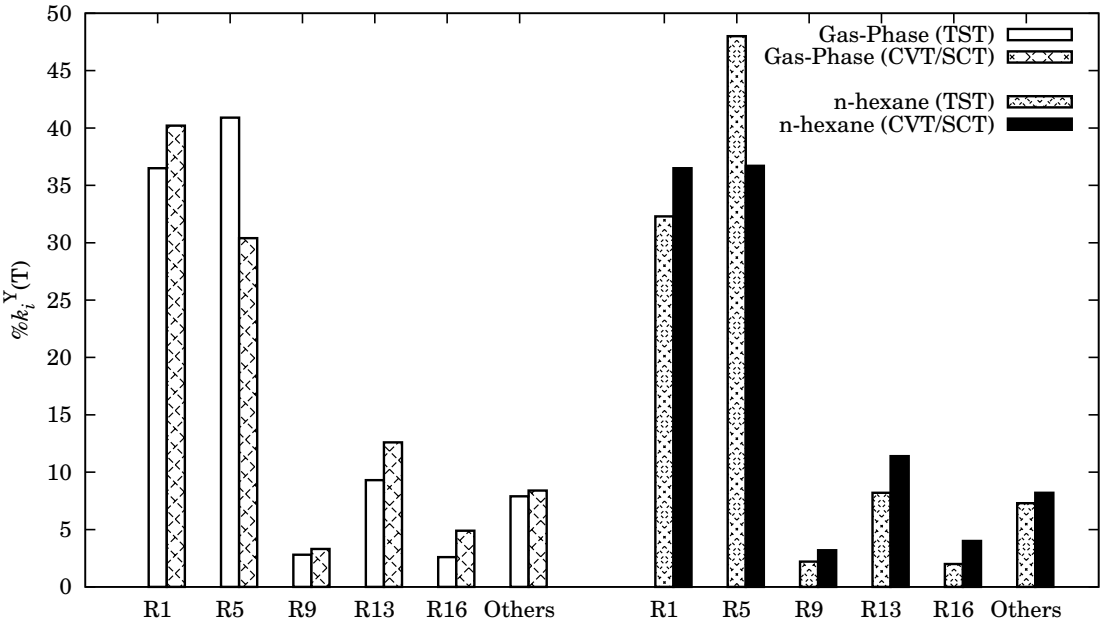
Gas-Phase (TST)
Gas-Phase (CVT/SCT)
n-hexane (TST)
n-hexane (CVT/SCT)
$\%k_i^Y(T)$
0
5
10
15
20
25
30
35
40
45
50
R1
R5
R9
R13
R16
Others
R1
R5
R9
R13
R16
Others

Figure 1

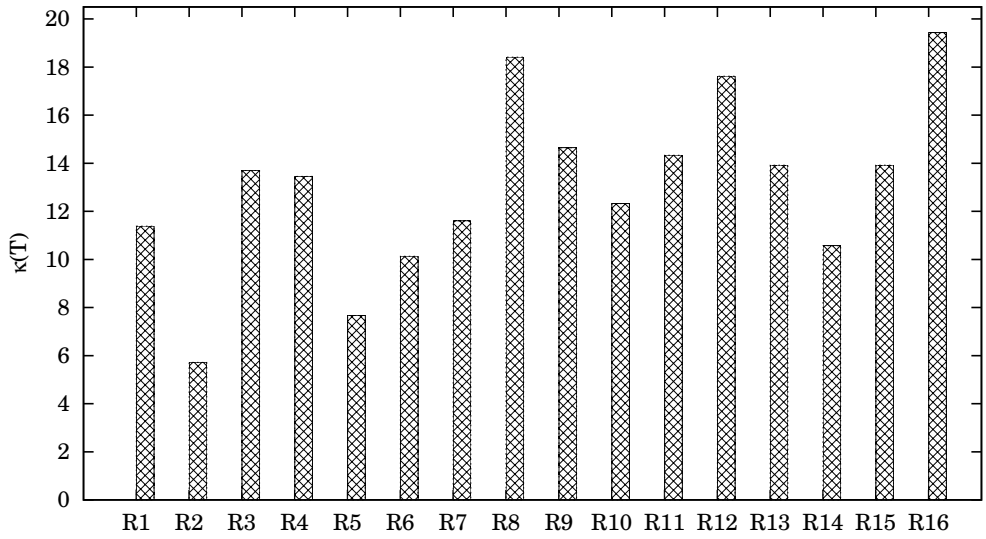
κ(T)
0
2
4
6
8
10
12
14
16
18
20
R1
R2
R3
R4
R5
R6
R7
R8
R9
R10
R11
R12
R13
R14
R15
R16

Figure 2

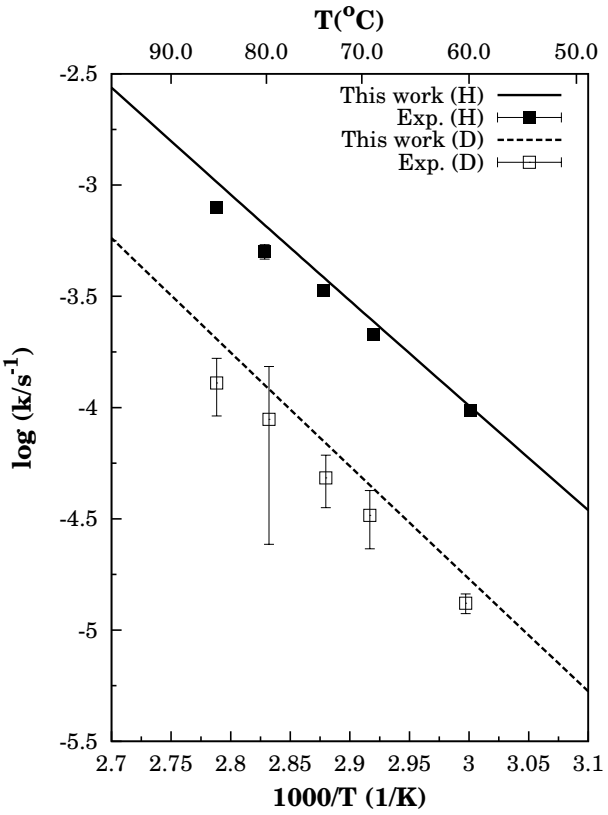
T(°C)
90.0
80.0
70.0
60.0
50.0
-2.5
-3
-3.5
-4
-4.5
-5
-5.5
log (k/s-1)
This work (H)
Exp. (H)
This work (D)
Exp. (D)
2.7
2.75
2.8
2.85
2.9
2.95
3
3.05
3.1
1000/T (1/K)

Figure 3

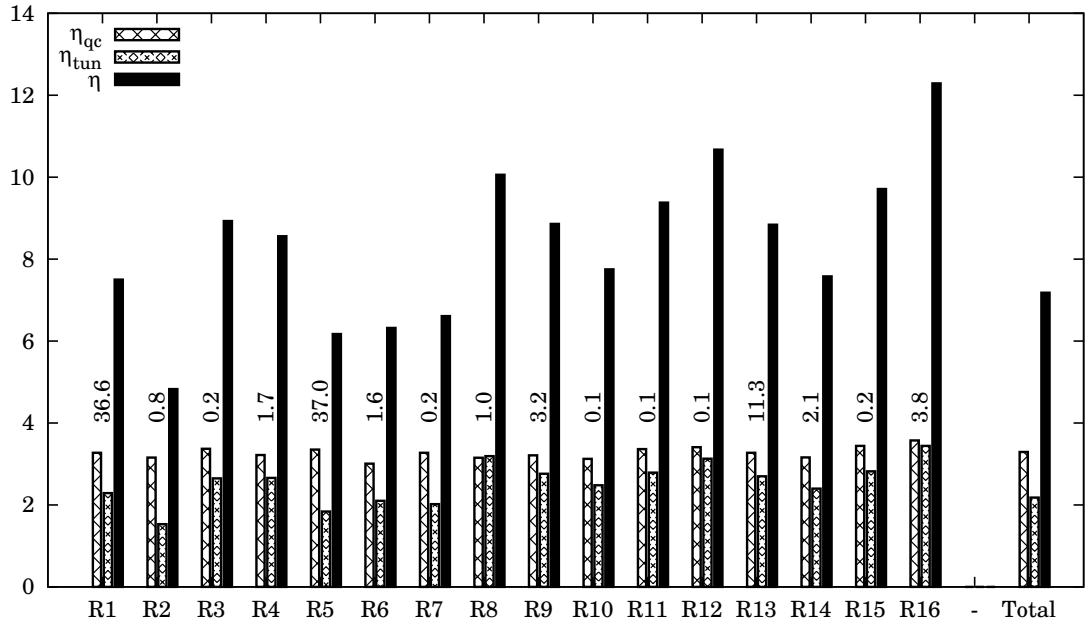
η_{qc}
η_{tun}
η
14
12
10
8
6
4
2
0
36.6
0.8
0.2
1.7
37.0
1.6
0.2
1.0
3.2
0.1
0.1
0.1
11.3
2.1
0.2
3.8
R1
R2
R3
R4
R5
R6
R7
R8
R9
R10
R11
R12
R13
R14
R15
R16
-
Total

Figure 4